

Journal Pre-proofs

Design, synthesis, and biological evaluation of hydroxamic acid-substituted 2,4-diaryl aminopyrimidines as potent EGFR T790M/L858R inhibitors for the treatment of NSCLC

Lixue Chen, Yunhao Zhang, Changyuan Wang, Zeyao Tang, Qiang Meng, Hunjun Sun, Yan Qi, Xiaodong Ma, Lei Li, Yanxia Li, Youjun Xu

PII: S0045-2068(21)00422-3
DOI: <https://doi.org/10.1016/j.bioorg.2021.105045>
Reference: YBIOO 105045

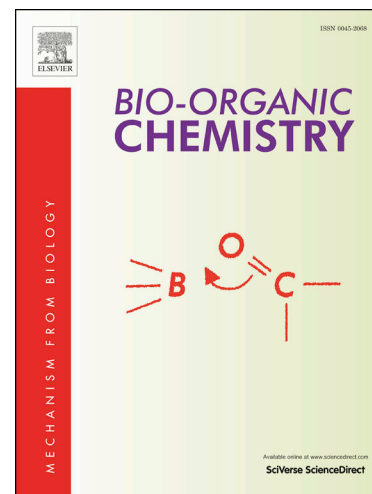
To appear in: *Bioorganic Chemistry*

Received Date: 3 March 2021
Revised Date: 15 May 2021
Accepted Date: 26 May 2021

Please cite this article as: L. Chen, Y. Zhang, C. Wang, Z. Tang, Q. Meng, H. Sun, Y. Qi, X. Ma, L. Li, Y. Li, Y. Xu, Design, synthesis, and biological evaluation of hydroxamic acid-substituted 2,4-diaryl aminopyrimidines as potent EGFR T790M/L858R inhibitors for the treatment of NSCLC, *Bioorganic Chemistry* (2021), doi: <https://doi.org/10.1016/j.bioorg.2021.105045>

This is a PDF file of an article that has undergone enhancements after acceptance, such as the addition of a cover page and metadata, and formatting for readability, but it is not yet the definitive version of record. This version will undergo additional copyediting, typesetting and review before it is published in its final form, but we are providing this version to give early visibility of the article. Please note that, during the production process, errors may be discovered which could affect the content, and all legal disclaimers that apply to the journal pertain.

© 2021 Published by Elsevier Inc.



Design, synthesis, and biological evaluation of hydroxamic acid-substituted 2,4-diaryl aminopyrimidines as potent EGFR^{T790M/L858R} inhibitors for the treatment of NSCLC

Lixue Chen^a, Yunhao Zhang^a, Changyuan Wang^a, Zeyao Tang^a, Qiang Meng^a, Hunjun Sun^a, Yan Qi^a, Xiaodong Ma^a, Lei Li^{a,*}, Yanxia Li^{b,*} and Youjun Xu^{c,*}

^a College of Pharmacy, Dalian Medical University, Dalian, 116044, PR China.

^b Department of Respiratory Medicine, The First Affiliated Hospital of Dalian Medical University, Dalian, PR China.

^c School of Pharmaceutical Engineering, and Key Laboratory of Structure-Based Drug Design & Discovery (Ministry of Education), Shenyang Pharmaceutical University, Shenyang, 110016, PR China.

* Corresponding author.

Email address: lilei0332@126.com (L. Li); liyanxia001@163.com (Y. Li); xuyoujun@syphu.edu.cn (Y. Xu).

Highlights

- Diphenylpyrimidine derivatives bearing hydroxamic acid group were designed and synthesized as potent EGFR^{T790M/L858R} inhibitors.
- **10j** demonstrated stronger inhibitory potency against EGFR^{T790M/L858R} than that of AZD-9291.
- **10j** displayed extremely selective inhibitory effects on H1975 cell lines (EGFR^{T790M/L858R}) over A431 cell lines (EGFR^{WT}).
- **10j** could block the cell cycle of H1975 cell lines at the G2/M stage.
- **10j** significantly suppressed tumour growth in xenograft mouse model.

Abstract

A series of 2,4-diarylaminopyrimidine derivatives bearing hydrophilic hydroxamic acids were designed and synthesized as potent EGFR^{T790M/L858R} inhibitors. Among the derivatives synthesized, **10c** (IC₅₀ = 5.192 nM), **10j** (IC₅₀ = 10.35 nM), and **10o** (IC₅₀ = 0.3524 nM) exhibited higher potencies against EGFR^{T790M/L858R} compared to the known EGFR inhibitor AZD-9291 (IC₅₀ = 20.80 nM). Moreover, **10j** showed moderate activity against H1975 cells transfected with the EGFR^{T790M/L858R}

mutant, with an IC_{50} of 0.2113 μ M over A431 (wild-type EGFR, $SI = 47.3$). In addition, **10j** exhibited low toxicity in normal HBE cells (human bronchial epithelial cells, $IC_{50} > 40 \mu$ M). Analysis of the mode of action indicated that **10j** effectively induced apoptosis in H1975 cells by arresting the cells in the G2/M phase. Compound **10j** also demonstrated efficacy in inhibiting tumor growth in a murine H1975 xenograft mouse model without losing body weight or killing the mice. Taken together, these results suggested that **10j** might be a promising candidate for development as a potential treatment for NSCLC harboring the EGFR^{T790M/L858R} mutation.

Key words: NSCLC; EGFR T790M/L858R; resistance; inhibitors

1. Introduction

Non-small cell lung cancers (NSCLC) harboring somatic activating mutations in the tyrosine kinase domain of the epidermal growth factor receptor (EGFR) are well-studied examples of oncogene addiction [1]. EGFR is a transmembrane glycoprotein belonging to the human epidermal growth factor receptor (HER) family that is essential in cell signaling pathways implicated in cell proliferation, differentiation, and apoptosis [2,3]. EGFR mutations are the first driver alterations characterized in NSCLC and are found in approximately 10–15% of non-Asian and 48% of Asian patients [1,4–5]. The most common oncogenic mutations in NSCLCs are small, in-frame deletions in exon 19 and a L858R point mutation, both of which likely cause constitutive activation of the tyrosine kinase domain by destabilizing the autoinhibited conformation [6–9]. First-generation EGFR inhibitors Gefitinib (**1**) [10] and Erlotinib (**2**) [11] (**Fig. 1**) were suitably efficacious in patients suffering from NSCLC with sensitizing EGFR mutations (both exon 19 deletions and L858R).

Unfortunately, after administration of the first-generation drugs for 10–14 months, the cancers in approximately 60% of the patients became gradually exacerbated [12, 13]. The presence of the T790M gatekeeper mutation increased the affinity of ATP binding in the ATP-binding pocket of the receptor, thereby outcompeting the EGFR inhibitors for binding and reducing their efficacies against the receptor [14]. Second- and third-generation EGFR inhibitors, which functioned as irreversible inhibitors that targeted the formation of covalent adducts with Cys797, were developed to increase the potency of binding against the T790M/L858R mutants [15]. However, due to the narrow selectivity window between wild-type EGFR (EGFR^{WT}) and the mutants, patients who were administered second-generation EGFR inhibitors, such as BIBW-2992 (3) [16] and HKI-272 (4) [17], suffered from adverse side effects in the clinic [18]. To improve the safety profiles of the second-generation inhibitors, third-generation EGFR inhibitors, such as WZ4002 (5) [19], AZD-9291(6) [20], Almonertinib (7) [21], and other structurally related compounds that are selective against the dominant mutants, have been developed in recent years. Among them, AZD-9291 (Osimertinib) was approved by U.S. Food and Drug Administration (FDA) to be used for treating EGFR T790M/L858R mutation NSCLC in 2015, and Almonertinib was approved by the National Medical Products Administration (NMPA) in 2020.

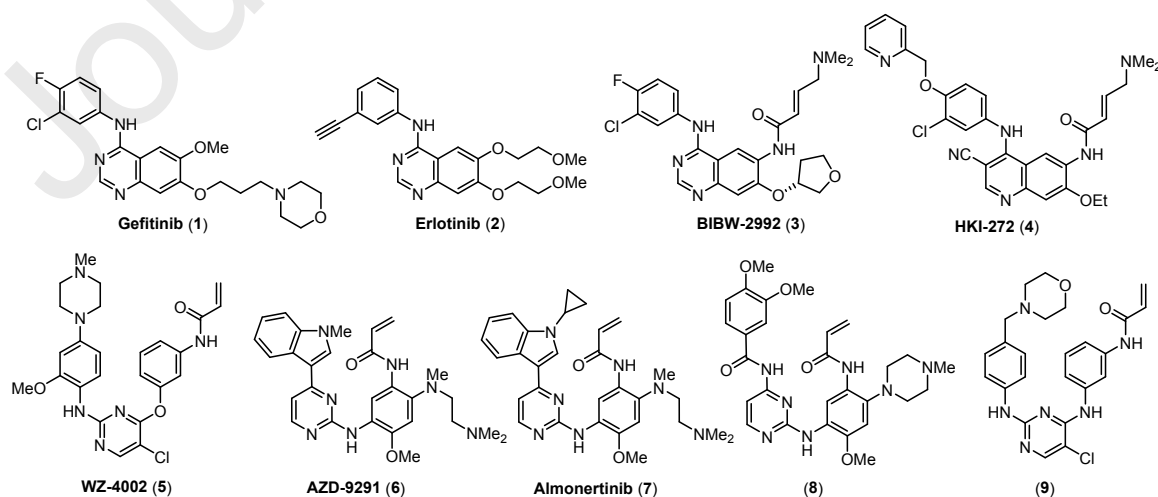
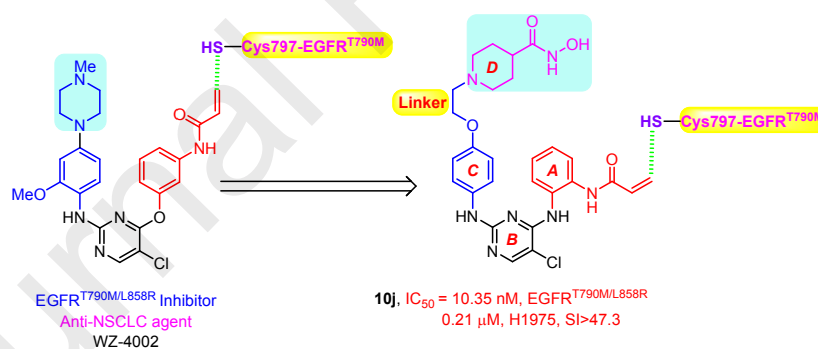


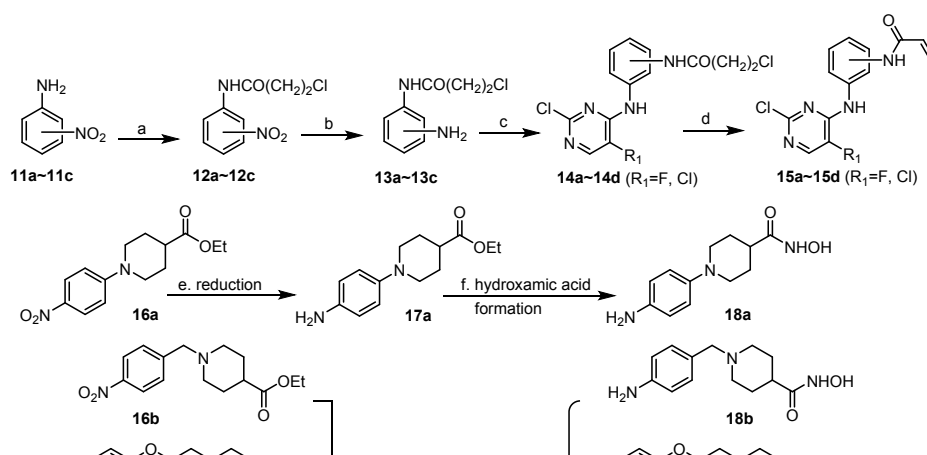
Fig. 1. Chemical structures of some novel EGFR inhibitors.

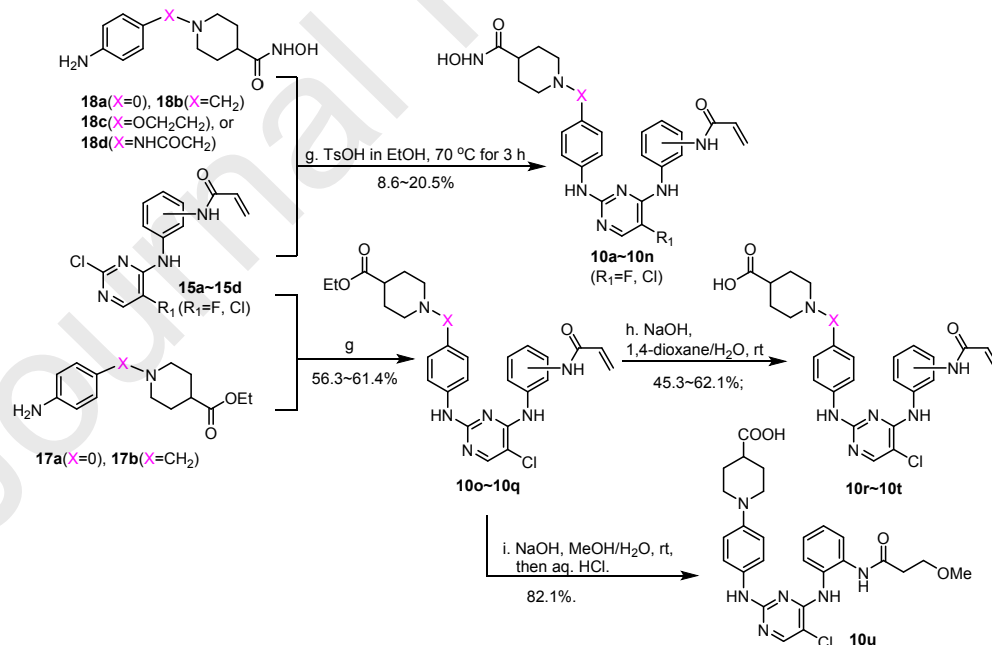
Our group has spent a considerable amount of time on the discovery of novel mutant-selective inhibitors against EGFR^{T790M/L858R} by modifying the solution region of lead compounds such as **8** [22] and **9** [23]. The SAR results of the scaffold of these lead compounds [23, 24] indicated that the 2,4-diarylaminopyrimidine scaffold was very hydrophobic, so the introduction of hydrophilic groups onto Ring D, as well as the extension of the linker between Rings C and D, could be effective for improving the druglikeness and the binding activity of the scaffold. Herein, a series of 2,4-diarylaminopyrimidine derivatives featuring hydrophilic isohydroxamic acid and carboxylic acid groups were designed, synthesized, and evaluated by *in vitro* kinase enzymatic and cellular activity assays and an *in vivo* xenograft mouse model in an effort to identify more effective and selective inhibitors against EGFR^{T790M/L858R} (**Fig. 2**).

**Fig. 2.** Strategy for the design of the target 2,4-diarylaminopyrimidine derivatives.

2. Results and Discussion

2.1 Chemistry



Scheme 1. Synthesis of intermediates **15a–d** and **18a–d**.Scheme 2. Synthesis of compounds **10a–u**.

The synthesis of the designed 2,4-diarylamino pyrimidine derivatives **10a–u** is shown in **Schemes 1–2**. Briefly, the commercially available substrates **11a–c** were coupled to 3-chloropropionyl chloride *via* a trivial acyl substitution reaction to afford intermediates **12a–c**. Subsequently, the nitroarene group in compounds **12a–c** was reduced to the corresponding aniline by H_2 in the presence of 10% Pd/C to form intermediates **13a–c**, which then underwent condensation reactions with 2,4,5-trichloropyrimidine or 2,4-dichloro-5-fluoropyrimidine to generate intermediates **14a–d**. The α , β -elimination was finally carried out to produce the key intermediates **15a–d** containing the acrylamide pharmacophore. After reduction of the NO_2 group in **16a–d** to the corresponding anilines, **18a–d** were synthesized by nucleophilic substitution with hydroxylamine hydrochloride in the presence of CH_3ONa . Finally, the final compounds **10a–q** were synthesized by nucleophilic aromatic substitution of the aryl chloride moiety of **15a–d** with the aniline group of **17a–b/18a–d** catalyzed by TsOH. In addition, final compounds **10r–t** were prepared after hydrolysis of the ester intermediates. Lastly, the negative control **10u** was synthesized by hydrolysis and Michael addition of **10o**.

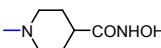
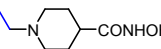
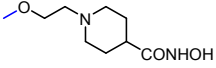
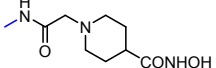
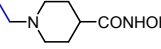
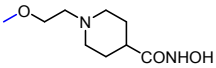
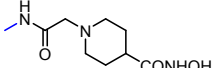
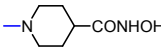
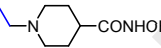
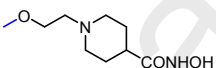
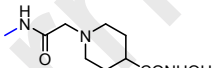
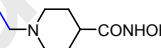
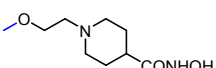
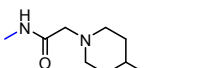
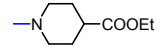
2.2 Biological activity

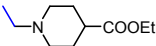
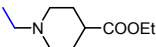
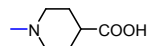
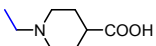
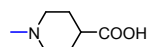
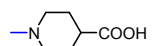
2.2.1 EGFR inhibitory activities and selectivity assays

Table 1. EGFR tyrosine kinase inhibitory activities of **10a–u** *in vitro*^a.



Compd.	R ₁	R ₂	R ₃	Enzymatic activity (IC ₅₀ , nM)		
				EGFR ^{T790M/L858R}	EGFR ^{WT}	SI

10a	Cl		3-NHCOCH=CH ₂	92.67	34.44	--
10b	Cl		3-NHCOCH=CH ₂	6.376	1.082	--
10c	Cl		3-NHCOCH=CH ₂	5.192	40.62	7.8
10d	Cl		3-NHCOCH=CH ₂	50.29	2.952	--
10e	F		3-NHCOCH=CH ₂	51.03	23.97	--
10f	F		3-NHCOCH=CH ₂	1.471	1.165	--
10g	F		3-NHCOCH=CH ₂	3.343	8.187	2.4
10h	Cl		2-NHCOCH=CH ₂	20.74	0.6554	--
10i	Cl		2-NHCOCH=CH ₂	13.88	17.81	1.3
10j	Cl		2-NHCOCH=CH ₂	10.35	65.86	6.4
10k	Cl		2-NHCOCH=CH ₂	9.199	6.035	--
10l	Cl		4-NHCOCH=CH ₂	5.198	9.218	1.8
10m	Cl		4-NHCOCH=CH ₂	1.636	0.1403	--
10n	Cl		4-NHCOCH=CH ₂	32.31	198.5	6.1
10o	Cl		2-NHCOCH=CH ₂	0.3524	60.52	171.3

10p	Cl		2-NHCOCH=CH ₂	6.863	1.517	--
10q	Cl		3-NHCOCH=CH ₂	5.602	45.44	8.1
10r	Cl		2-NHCOCH=CH ₂	165.9	2.081	--
10s	Cl		2-NHCOCH=CH ₂	7.401	326.0	44.1
10t	Cl		3-NHCOCH=CH ₂	117.5	189.2	1.6
10u	Cl		3-NHCO(CH ₂) ₂ OMe	>500	>500	--
AZD-9291				20.80	567.5	27.3

^a Dose-response curves were determined at three different concentrations. The IC₅₀ values are the concentrations in nanomolar needed to inhibit cell growth by 50% as determined from these curves.

All the targets were evaluated for their activities against EGFR^{WT} and EGFR^{T790M/L858R} using the ADP-GloTM kinase assay system, with AZD-9291 functioning as the control. The results represented in **Table 1** indicated that most of the targets displayed strong inhibitory activities against EGFR^{T790M/L858R}, with IC₅₀ values ranging from 0.3524 nM to 165.9 nM. Several of the targets, such as **10c** (IC₅₀ = 5.192 nM), **10j** (IC₅₀ = 10.35 nM), and **10o** (IC₅₀ = 0.3524 nM), exhibited tighter binding to EGFR^{T790M/L858R} than the EGFR inhibitor AZD-9291 as well as higher selectivity for EGFR^{T790M/L858R} over EGFR^{WT}. Moreover, compounds **10h–k**, which featured the acrylamide pharmacophore at the C''-2 position on Ring A, inhibited EGFR^{T790M/L858R} with IC₅₀ values ranging from 9.199 nM to 20.74 nM. The 2,4-diarylaminopyrimidine derivatives bearing ester groups as prodrugs of the carboxylic acids on Ring D had stronger potencies compared to the corresponding

carboxylic acids. However, replacement of the 5-chlorine on the pyrimidine core with a fluorine substituent (**10e–g**) was ineffective for improving the potency against EGFR^{T790M/L858R} and selectivity over EGFR^{WT}. Notably, **10u**, which did not contain an acrylamide group, weakly inhibited both EGFR^{T790M/L858R} and EGFR^{WT}, suggesting that the acrylamide moiety was necessary for activity in this scaffold.

2.2.2 Cellular inhibition and selectivity assays

Table 2. Cellular anti-proliferative activities of **10a–u** (IC₅₀, μM)^a.

Compd.	Anti-proliferative activity (IC ₅₀ , μM)							SI
	H1975	A431	A549	HBE	ASPC-1	H23	L-02	
10a	2.537	7.31	>1.25	14.7	2.245	7.204	2.42	2.88
10b	5.962	>10	>1.25	8.348	3.483	6.708	2.863	>1.68
10c	4.255	>10	>1.25	7.724	4.23	7.775	2.767	>2.35
10d	>40	>10	>1.25	15.43	>5	25.27	11.07	--
10e	9.556	>10	>1.25	7.812	>5	23.91	4.922	>1.05
10f	5.079	6.24	>1.25	5.249	>5	13.06	2.661	1.23
10g	>40	>10	>1.25	11.14	>5	25.67	23.66	--
10h	0.3653	>10	0.6543	>40	0.8001	0.6715	2.529	>27.4
10i	0.3114	6.856	0.5411	24.5	0.3594	<0.3125	4.364	22.0
10j	0.2113	>10	0.409	>40	0.5203	0.5251	3.058	>47.3
10k	0.3698	>10	>1.25	>40	0.7571	4.382	22.09	>27.0
10l	>40	9.947	>1.25	6.252	>5	16.43	9.293	--
10m	7.261	13.97	>1.25	6.775	4.533	6.928	4.759	1.92
10n	>10	>10	>1.25	37.65	>5	16.35	14.00	--
AZD-9291	0.091	1.226						

^a Dose-response curves were determined at five different concentrations. The IC₅₀ values are the concentrations in micromolar needed to inhibit cell growth by 50% as determined from these curves.

Table 3. Cellular anti-proliferative activities of **10o–u** (IC₅₀, μM)^a.

Compounds	Anti-proliferative activity	
	(IC ₅₀ , μM)	
	H1975	L-02
10o	0.6884	19.52
10p	0.5731	4.909
10r	0.8183	4.171
10s	3.145	13.31
10t	1.154	9.511
10u	>40	19.52
AZD-9291	0.091	--

^a Dose-response curves were determined at five different concentrations. The IC₅₀ values are the concentrations in micromolar needed to inhibit cell growth by 50% as determined from these curves.

The antiproliferative activities of **10a–n** and the positive control AZD-9291 were investigated in the NSCLC cell lines A431 EGFR^{WT}, H1975 EGFR^{T790M/L858R}, A549^{KRAS G12S} and H23^{KRAS mutant}, as well as a human metastatic pancreatic adenocarcinoma cell line (Aspc-1) and a normal cell line (HBE), using the CCK-8 assay (**Table 2**). The results of the cell-based anti-proliferative activity assays indicated that most of the 2,4-diarylaminopyrimidine derivatives strongly inhibited the proliferation of the H1975 cells, with the IC₅₀ values of some of these derivatives in the nanomolar regime, such as **10h** (IC₅₀ = 0.3653 μM), **10i** (IC₅₀ = 0.3114 μM), **10j** (IC₅₀ = 0.2113 μM), and **10k** (IC₅₀ = 0.3698 μM). These four analogs were also highly selective for EGFR^{T790M/L858R} in the H1975 cells over EGFR^{WT} in the A431 cell line, with selectivity indices (SI) > 22, all of which were higher than the positive control. Higher selectivities indicated that the inhibitors more weakly inhibited normal cell EGFR expression compared to the mutants, which is advantageous for mitigating the side effects associated with targeting the entire EGFR network.

The most obvious SAR trend of the 2,4-diarylaminopyrimidines obtained by the cell-based activity assays was that the substitution of the acrylamide pharmacophore on Ring A noticeably improved the anti-proliferation activities of the derivatives. When the acrylamide remained in the 3-position of Ring A, extending the linker between Rings C and D was able to effectively increase the anti-proliferative activity of the derivatives in the H1975 cell line. For example, substitution of the group with an ethoxy piperidine linker was the most effective for enhancing the anti-proliferative activity, such as in **10c** ($IC_{50} = 4.255 \mu\text{M}$), **10f** ($IC_{50} = 5.079 \mu\text{M}$), and **10j** ($IC_{50} = 0.2113 \mu\text{M}$). However, when this linker was an acetamide, such as in compounds **10d**, **10g**, and **10n**, the compounds exhibited reduced activity against H1975. Meanwhile, the 2,4-diarylaminopyrimidines analogs featuring esters and carboxylic acid (**10o–u**) inhibited the proliferation of the H1975 and L-02 cell lines. For example, compounds **10o** ($IC_{50} = 0.6884 \mu\text{M}$) and **10p** ($IC_{50} = 0.5731 \mu\text{M}$) strongly inhibited cellular proliferation in H1975 cells and did not demonstrate selectivity for the kinase domain; however, the substitution of these groups with hydroxamic acid groups led to an enhancement in the anti-proliferative activity of this scaffold (**Table 3**). Measuring the toxicity of drugs in host cells is important for assessing the safety of the candidates early in the drug discovery process. Most of the 2,4-diarylaminopyrimidines analogs exhibited weak inhibition against normal HBE and L-02 cells. In particular, the most active inhibitor **10j** had the highest selectivity index ($SI > 47.3$) of all the analogs, and it also exhibited weak inhibition against the proliferation of HBE ($IC_{50} > 40 \mu\text{M}$) and L-02 ($IC_{50} = 3.058 \mu\text{M}$) cells, indicating potential for further development. Meanwhile, **10h**, **10i**, and **10j** also strongly inhibited the proliferation of the KRAS mutant lung cancer A549 and

H23 cell lines and the pancreatic cancer ASCP-1 cell line, suggesting that the targets might have multi-target effects.

2.2.3 Migration inhibition assay

After evaluation of the EGFR inhibitory activities and selectivity of the 2,4-diarylaminopyrimidines analogs **10a–u**, **10j** was selected for further studies. Wound-healing assays were conducted to determine if different concentrations (0.25, 1, and 4 μM) of **10j** could influence the migration of H1975 cells 0, 24, 48 h after scratching the cell monolayer (**Fig. 3**). As expected, the DMSO control vehicle promoted the strongest migration of the H1975 cells. Under the same conditions, H1975 cell migration in the **10j**-treated groups was significantly lower than in the control group. Therefore, the results of the wound healing assay indicated that **10j** could effectively inhibit the migration and invasion of H1975 cells.

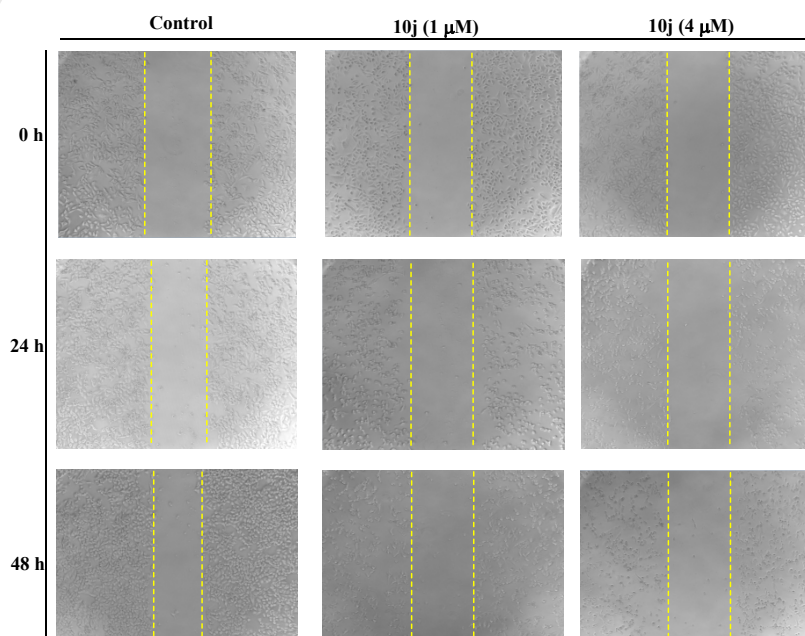
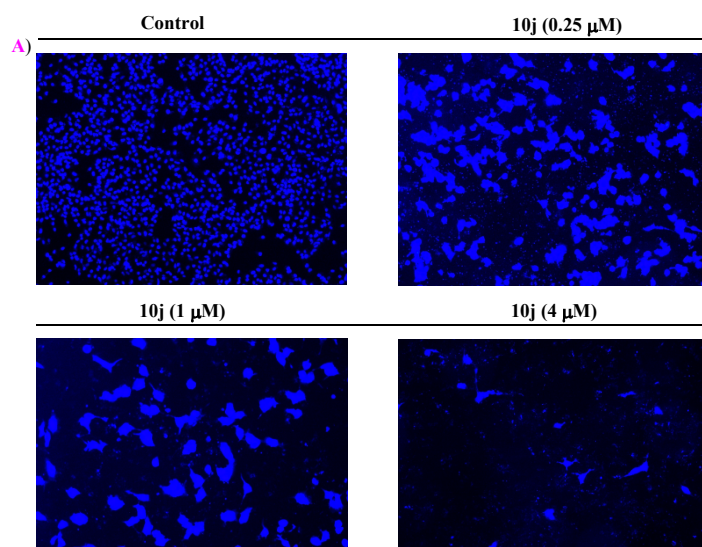


Fig. 3. Representative images of the H1975 cells treated with different concentrations of **10j** for 0, 24, and 48 h during the wound-healing assay.

2.2.4 Morphological staining analysis

The analysis of the morphology change of H1975 cells were carried out using DAPI staining. As shown in **Fig. 4A**, H1975 bearing EGFR T790M/L858R-mutated exposed with **10j**, chromatin condenses and nuclear disintegration were observed subsequent to DAPI staining. Under natural light, the proportion of abnormal cells, such as fusiform and sickle type, increased significantly (**Fig. 4B**). All of the phenomena was the characteristics of apoptotic programmed cell death.



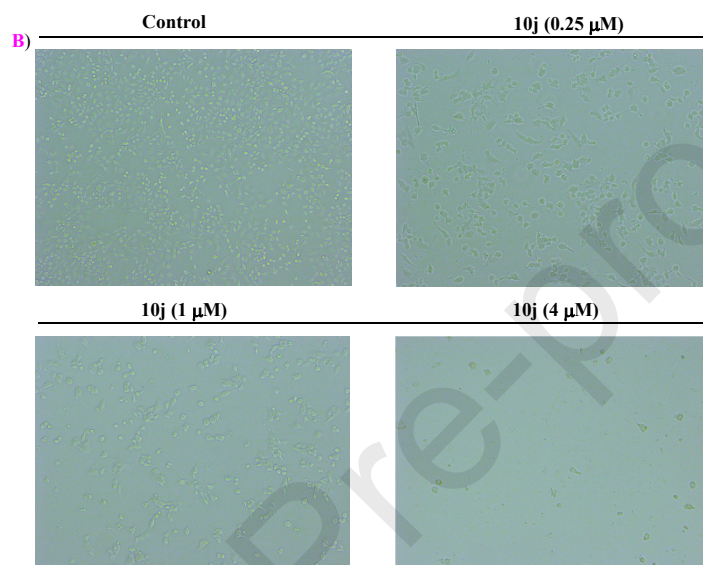


Fig. 4. Morphological changes of the H1975 cells (100x final magnification). A): DAPI staining of the H1975 cells treated with different concentrations (0.25, 1, and 4 μM) of **10j** for 72 h; B): Under nature light, H1975 cells treated with different concentrations (0.25, 1, and 4 μM) of **10j** for 72 h.

2.2.5 Flow cytometry analysis

To characterize the propensity of **10j** to induce apoptosis, flow cytometry was performed on the H1975 cell lines using Annexin V-PI as the indicator of apoptosis. After incubating the H1975 cells with **10j** at concentrations ranging from 0.5 to 2.0 μM for 48 h, the percentage of apoptotic cells dramatically increased from 15.99% to 21.29% (**Fig. 5A**). Correspondingly, compared to the control

group, the percentage of the H1975 cells in G0/G1 phase significantly decreased from 40.32% to 18.38% in a dose-dependent manner, while the percentage of cells in the G2/M phase increased from 46.38% to 65.85% at a concentration of 0.15 μM). However, the proportion of H1975 cells in S phase essentially remained unchanged in the concentration range tested (**Fig. 5B**). Therefore, the flow cytometry results indicated that **10j** mainly arrested the H1975 cells in the G2/M stage in a concentration-dependent manner.

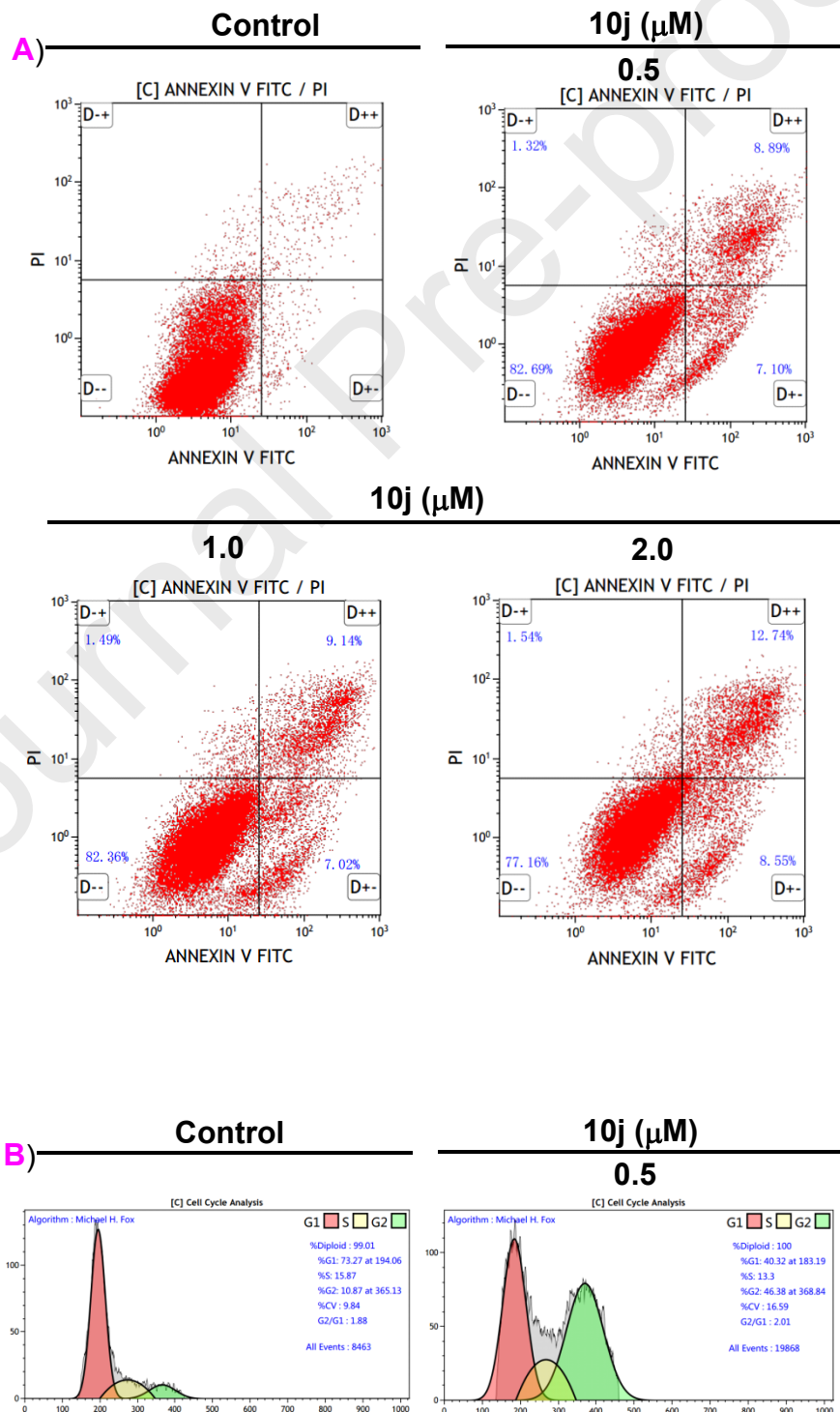


Fig. 5. A) **10j**-induced H1975 cell apoptosis. B) Effects of **10j** on H1975 cell-cycle arrest determined by flow cytometry.

2.2.6 *In vivo antitumor activity*

Due to its potent inhibitory activity against EGFR^{T790M/L858R} and H1975 proliferation, as well as a low toxicity in normal cells, **10j** was further evaluated for antitumor efficacy *in vivo* using a xenograft mouse model of EGFR^{T790M/L858R}-driven human NSCLC cells. Severe combined immunodeficient (SCID) mice harboring established H1975 tumor xenografts were orally dosed with **10j** at 50 mg/kg daily over a 14-day period. Tumor growth slowed down noticeably at this dosage, such that the tumor weight decreased by ~80% after the 14 days (**Fig. 6**). In addition, there was no mortality or significant loss of body weight (< 5% relative to the vehicle-matched controls) during treatment.



Fig. 6. *In vivo* effects of **10j** on the tumor growth of H1975 cell xenografts in nude mice. (A) Images of the tumors collected from the mice; (B) tumor weight; data are presented as the mean \pm SD ($n = 4$). * $p < 0.05$ and ** $p < 0.01$ compared to the control group.

2.3 Molecular modeling

To better understand the interactions between **10j** and EGFR^{T790M/L858R}, molecular docking studies of **10j** in the ATP-binding site of EGFR^{T790M/L858R} (PDB: 3IKA) were conducted using the software AutoDock 4.2. As shown in **Fig. 7**, both **10j** and the known EGFR inhibitor WZ4002 exhibited tight interactions with the residues in the active site of EGFR^{T790M/L858R} in a U-shape, while the binding conformation of **10j** was reversed compared to WZ4002. The C"-2 acrylamide functionality on Ring A of **10j** formed hydrogen bond interactions with Cys797 (closer in space), which enabled Michael additions of the Cys797 sulfhydryl group onto the acrylamide to form a covalent adduct with the receptor. The docking studies revealed that acrylamide pharmacophore in **10h**, **10i**, **10j**, and **10k** was essential for promoting the inhibition of cellular proliferation by irreversibly inhibiting the EGFR^{T790M/L858R} receptor. In addition, strong hydrogen bonding interactions were observed between the N-1 of the pyrimidine core of WZ4002 and Met793 in the kinase hinge of the receptor as well as between the 2-aminopyrimidine NH of **10j** and Met793.

Furthermore, hydrophobic interactions between Leu718 and Rings B and C of **10j**, as well as between Leu844 and Rings C and D of **10j**, were observed. These molecular docking results were consistent with the empirical data obtained from the biological assays, and they provided a structural basis for further rational design of EGFR^{T790M/L858R} inhibitors.

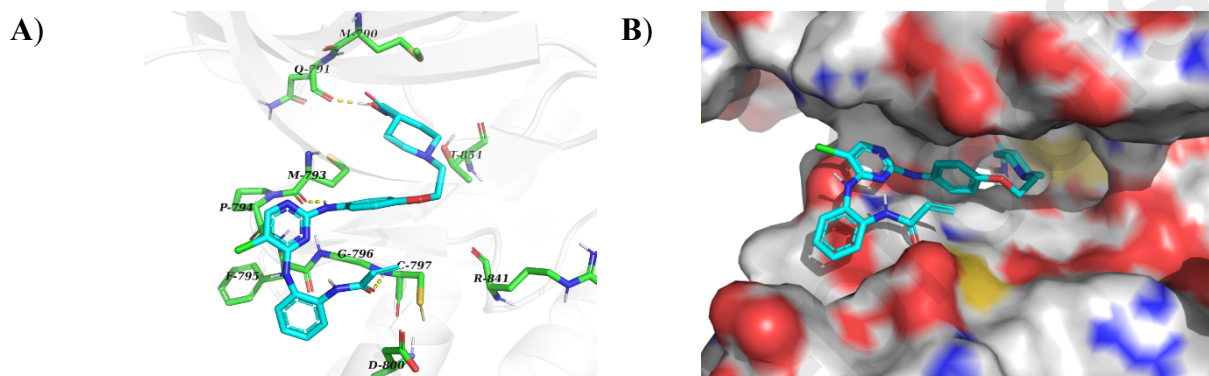


Fig. 7. Putative binding mode of **10j** with EGFR^{T790M/L858R}. (A) Detailed interactions with the protein residues. Each dashed yellow line represents hydrogen bonds. (B) Three-dimensional space matching diagram of **10j** and the active site.

Fig. 7. Putative binding mode of **10j** in the ATP-binding site of EGFR^{T790M/L858R}. (A) Detailed interactions with the residues in the active site of the receptor. Each dashed yellow line represents hydrogen bonds. (B) Three-dimensional space matching diagram of **10j** in the active site.

3. Conclusion

A series of diphenylpyrimidine derivatives bearing hydroxamic acid groups was designed and synthesized as potent and selective inhibitors of EGFR^{T790M/L858R} over EGFRTM. Among them, **10j** was identified as the most promising lead compound and was found to strongly inhibit the EGFR^{T790M/L858R} mutated kinase with an IC₅₀ value of 10.35 nM. In addition, it moderately suppressed

the proliferation of H1975 cells transfected with the EGFR^{T790M/L858R} mutant with an IC₅₀ value of 0.2113 μM over A431 (EGFR^{WT}, IC₅₀ > 10 μM). Meanwhile, **10j** also exhibited lower toxicity in normal HBE and L-02 cells, indicating an improved administration safety margin. Moreover, **10j** induced apoptosis by arresting the H1975 cells in the G2/M phase. The lead **10j** also displayed anti-cancer efficacy in an H1975-driven xenograft mouse model *in vivo*. Overall, these results suggested that **10j** might be promising as a potent and selective EGFR^{T790M/L858R} inhibitor for further development.

4. Experimental section

4.1 General methods and chemistry

Unless otherwise noted, commercial solvents and reagents were used without further purifications. High resolution ESI-MS was performed on an Agilent 1100 HPLC/MS system. ¹H NMR and ¹³C NMR spectra on a Bruker AV 400 MHz spectrometer were recorded in DMSO-*d*. Coupling constants (*J*) are expressed in hertz (Hz). Chemical shifts (*δ*) of NMR are reported in parts per million (ppm) units relative to internal control (TMS). All reactions were monitored by TLC, using silica gel plates with fluorescence GF254 and UV light visualization. Flash chromatography separations were obtained on Silica Gel (300~400 mesh) using dichloromethane/methanol as eluents.

4.2 General procedure for the synthesis of **10a~u**

4.2.1 General procedure for the synthesis of **10a~n**

A mixture of **11a~c** (50 mmol) and potassium carbonate (50 mmol) in acetonitrile was gradually added 3-chloropropanoyl chloride (100 mmol) under argon. After the addition, it was allowed to

warm to room temperature, and continuously stirred for 60 min. The mixture was diluted with ethyl acetate and brine, the separated organic layer was washed with brine and dried over anhydrous Na₂SO₄. After removing the organic solvent under vacuum, the rest of organic substance was dispersed with petroleum ether to give the crude. **12a~c** (40 mmol), Pd-C (5% w/w) were added to methanol, catalytic hydrogenation was carried out at room temperature for 10 hours. Pd-C was filtered out and the organic phase was vacuum distilled to obtain **13a~c**. **13a~c** (30 mmol), 2,4,5-trichloropyrimidine/2,4-dichloro-5-fluoropyrimidine (30 mmol) and DIPEA (60 mmol) in acetonitrile, it was gradually heated to 80 °C and stirred for 10 h. The precipitate was filtrated and washed with water, and the acquired production could directly be used without further purification. Finally, a mixture of **14a~d** (25 mmol), TEA (200 mmol) and MeCN was stirred under refluxing for 6 h. Then water was gradually added to the cooled mixture and stirred for 30 min to allow the final target **15a~d** precipitated from the mixture.

16a~d and the corresponding reduced amine intermediate were prepared according to the reported process [25–28]. Argon atmosphere, **17a~d** (25 mmol) and hydroxylamine (0.125 mol) in anhydrous methanol, sodium methoxide (0.15 mol) in methanol solution was slowly added to the mixture. After the addition, the reaction was allowed to warm room temperature and stirred for 2 h. Adjusted pH to 6 with dilute hydrochloric acid, the inorganic salt was removed by filtration and the rest of organic phase was vacuum distilled to produce the **18a~d**.

A mixture of **15a~d** (3.0 mmol), **18a~d** (1.5 mmol), and *p*-TsOH (4.5 mmol) in *n*-BuOH was gradually heated to 70 °C and stirred for 3 h. After reaction, the solvent was vacuum distilled and the

residuum was dispersed with saturated sodium bicarbonate/ethyl acetate. The organic was vacuum distilled to give the crude which was purified by (Prep-HPLC) to get the **10a~n**.

4.2.1.1 *1-(4-((4-((3-acrylamidophenyl)amino)-5-chloropyrimidin-2-yl)amino)phenyl)-N-hydroxy piperidine-4-carboxamide (10a)*

Yield 19.6%; off-white solid. ^1H NMR(400 MHz, $\text{DMSO}-d_6$): δ 10.46(s, 1H), 10.19(s, 1H), 9.08(s, 1H), 8.85(s, 1H), 8.73(s, 1H), 8.09(s, 1H), 7.86(s, 1H), 7.55(d, $J=7.08$ Hz, 1H), 7.44(d, $J=8.34$ Hz, 2H), 7.30(t, $J=7.74$ Hz, 2H), 6.71(d, $J=7.02$ Hz, 2H), 6.47(dd, $J=16.86, 10.14$ Hz, 1H), 6.28(d, $J=16.86$ Hz, 1H), 5.77(d, $J=10.14$ Hz, 1H), 3.53–3.51(m, 2H), 2.50–2.48(m, 2H), 2.11–2.06(m, 1H), 1.71–1.66(m, 4H); ^{13}C NMR(100 MHz, $\text{DMSO}-d_6$): δ 171.86, 163.56, 158.28, 156.54, 155.25, 146.68, 139.45, 139.33, 132.94, 132.40, 129.03, 127.32, 120.60(2C), 119.47, 116.78(2C), 115.88, 115.75, 103.42, 49.74(2C), 40.67, 28.61(2C). HRMS (ESI⁺) for $\text{C}_{25}\text{H}_{26}\text{ClN}_7\text{O}_3$, $[\text{M}+\text{Na}]^+$ calcd: 530.1678, found: 530.1666.

4.2.1.2 *1-(4-((4-((3-acrylamidophenyl)amino)-5-chloropyrimidin-2-yl)amino)benzyl)-N-hydroxy piperidine-4-carboxamide (10b)*

Yield 10.2%; off-white solid. ^1H NMR(400 MHz, $\text{DMSO}-d_6$): δ 10.40(s, 1H), 10.24(s, 1H), 9.34(s, 1H), 8.93(s, 1H), 8.69(s, 1H), 8.14(s, 1H), 7.93(s, 1H), 7.57–7.53(m, 3H), 7.32–7.30(m, 2H), 7.04(d, $J=7.45$ Hz, 2H), 6.48(dd, $J=16.84, 10.27$ Hz, 1H), 6.27(d, $J=16.84$ Hz, 1H), 5.77(d, $J=10.27$ Hz, 1H), 3.35(s, 2H), 2.81(d, $J=10.02$ Hz, 2H), 1.99–1.93(m, 1H), 1.93–1.87(m, 2H), 1.63–1.57(m, 4H); ^{13}C NMR(100 MHz, $\text{DMSO}-d_6$): δ 171.89, 163.63, 158.12, 156.61, 155.22, 139.82, 139.59, 139.30, 132.41, 130.52, 129.55(2C), 129.00, 127.28, 119.61, 119.07(2C), 115.88, 115.67, 104.22,

62.21, 52.77(2C), 40.00, 28.61(2C). HRMS (ESI⁺) for C₂₆H₂₈ClN₇O₃, [M+H]⁺ calcd: 522.2015, found: 522.2054.

4.2.1.3 *1-(2-(4-((4-((3-acrylamidophenyl)amino)-5-chloropyrimidin-2-yl)amino)phenoxy)ethyl)-N-hydroxypiperidine-4-carboxamide (10c)*

Yield 15.1%; off-white solid. ¹H NMR(400 MHz, DMSO-*d*₆): δ 10.39(s, 1H), 10.20(s, 1H), 9.14(s, 1H), 8.88(s, 1H), 8.69(s, 1H), 8.09(s, 1H), 7.89(s, 1H), 7.50(d, *J*=8.36 Hz, 1H), 7.48(d, *J*=8.52 Hz, 2H), 7.30(t, *J*=7.61 Hz, 1H), 7.30(d, *J*=7.61 Hz, 2H), 6.69(d, *J*=7.62 Hz, 2H), 6.46(dd, *J*=16.91, 10.22 Hz, 1H), 6.27(dd, *J*=16.91, 1.26 Hz, 1H), 5.76(dd, *J*=10.22, 1.26 Hz, 1H), 3.93(t, *J*=5.40 Hz, 2H), 2.93(d, *J*=11.09 Hz, 2H), 2.62(t, *J*=5.40 Hz, 2H), 1.99–1.94(m, 3H), 1.64–1.58(m, 4H); ¹³C NMR(100 MHz, DMSO-*d*₆): δ 172.00, 163.59, 158.24, 156.58, 155.23, 153.67, 139.48, 139.33, 134.02, 132.35, 129.03, 127.32, 120.98(2C), 119.56, 115.90, 115.73, 114.56(2C), 103.68, 66.15, 57.39, 53.59(2C), 40.00, 28.91(2C). HRMS (ESI⁺) for C₂₇H₃₀ClN₇O₄, [M+Na]⁺ calcd: 574.1940, found: 574.1984.

4.2.1.4 *1-(2-((4-((4-((3-acrylamidophenyl)amino)-5-chloropyrimidin-2-yl)amino)phenyl)amino)-2-oxoethyl)-N-hydroxypiperidine-4-carboxamide (10d)*

Yield 11.6%; off-white solid. ¹H NMR(400 MHz, DMSO-*d*₆): δ 10.42(s, 1H), 10.18(s, 1H), 9.44(s, 1H), 9.26(s, 1H), 8.90(s, 1H), 8.70(s, 1H), 8.13(s, 1H), 7.96(d, *J*=8.56 Hz, 2H), 7.90(s, 1H), 7.49(d, *J*=7.74 Hz, 1H), 7.38(d, *J*=8.59 Hz, 2H), 7.36(d, *J*=7.57 Hz, 1H), 7.30(t, *J*=7.96 Hz, 1H), 6.46(dd, *J*=16.92, 10.14 Hz, 1H), 6.26(dd, *J*=16.92, 1.68 Hz, 1H), 5.75(dd, *J*=10.14, 1.68 Hz, 1H), 3.04(s, 2H), 2.88(d, *J*=10.96 Hz, 2H), 2.10(t, *J*=11.21 Hz, 2H), 1.99–1.95(m, 1H), 1.76–1.70(m, 2H),

1.60–1.58(m, 2H); ^{13}C NMR(100 MHz, $\text{DMSO}-d_6$): δ 171.96, 168.33, 163.63, 158.10, 156.55, 155.19, 139.60, 139.34, 136.59, 132.74, 132.38, 128.95, 127.30, 120.32(2C), 119.60, 119.52(2C), 115.75, 115.38, 104.11, 62.59, 53.32(2C), 40.49, 28.80(2C). HRMS (ESI⁺) for $\text{C}_{27}\text{H}_{29}\text{ClN}_8\text{O}_4$, $[\text{M}+\text{Na}]^+$ calcd: 587.1893, found: 587.1926.

4.2.1.5 *1-(4-((4-((3-acrylamidophenyl)amino)-5-fluoropyrimidin-2-yl)amino)benzyl)-N-hydroxy piperidine-4-carboxamide (10e)*

Yield 8.6%; off-white solid. ^1H NMR(400 MHz, $\text{DMSO}-d_6$): δ 10.39(s, 1H), 10.17(s, 1H), 9.43(s, 1H), 9.17(s, 1H), 8.69(s, 1H), 8.10(d, $J=3.48$ Hz, 1H), 7.97(s, 1H), 7.61(d, $J=7.98$ Hz, 2H), 7.49(d, $J=7.07$ Hz, 1H), 7.46(d, $J=8.14$ Hz, 1H), 7.28(t, $J=8.04$ Hz, 1H), 7.08(d, $J=7.74$ Hz, 2H), 6.47(dd, $J=16.93, 10.15$ Hz, 1H), 6.27(dd, $J=16.93, 1.56$ Hz, 1H), 5.77(dd, $J=10.15, 1.56$ Hz, 1H), 3.35(s, 2H), 2.85–2.77(m, 2H), 1.99–1.91(m, 1H), 1.91–1.78(m, 2H), 1.64–1.57(m, 4H); ^{13}C NMR(100 MHz, $\text{DMSO}-d_6$): δ 171.93, 163.60, 155.95(d, $J=1.73$ Hz), 150.25(d, $J=10.66$ Hz), 141.24(d, $J=19.15$ Hz), 141.07(d, $J=245.44$ Hz), 140.21, 139.56, 139.49, 132.42, 129.51(2C), 129.07, 127.25, 118.76(2C), 117.89, 115.29, 113.95, 62.32, 52.83(2C), 40.00, 28.69(2C). HRMS (ESI⁺) for $\text{C}_{26}\text{H}_{28}\text{FN}_7\text{O}_3$, $[\text{M}+\text{H}]^+$ calcd: 506.2310, found: 506.2327.

4.2.1.6 *1-(2-(4-((4-((3-acrylamidophenyl)amino)-5-fluoropyrimidin-2-yl)amino)phenoxy)ethyl)-N-hydroxypiperidine-4-carboxamide (10f)*

Yield 11.3%; off-white solid. ^1H NMR(400 MHz, $\text{DMSO}-d_6$): δ 10.41(s, 1H), 10.14(s, 1H), 9.38(s, 1H), 8.98(s, 1H), 8.72(s, 1H), 8.07(d, $J=3.12$ Hz, 1H), 7.94(s, 1H), 7.54(d, $J=8.52$ Hz, 2H), 7.49(d, $J=7.17$ Hz, 1H), 7.43(d, $J=7.61$ Hz, 1H), 7.28(t, $J=7.98$ Hz, 1H), 6.76(d, $J=8.50$ Hz, 2H),

6.47(dd, $J=16.88, 10.15$ Hz, 1H), 6.28(dd, $J=16.88$ Hz, 1H), 5.77(dd, $J=10.15$ Hz, 1H), 3.97(t, $J=5.64$ Hz, 2H), 2.97–2.95(m, 2H), 2.69–2.63(m, 2H), 2.02–1.97(m, 3H), 1.63–1.59(m, 4H); ^{13}C NMR(100 MHz, DMSO- d_6): δ 171.92, 163.57, 156.17(d, $J=1.80$ Hz), 153.49, 150.23(d, $J=10.78$ Hz), 141.27(d, $J=19.08$ Hz), 140.50(d, $J=245.93$ Hz), 139.55, 139.48, 134.54, 132.38, 129.09, 127.27, 120.75(2C), 117.84, 115.28, 114.67(2C), 113.96, 66.13, 57.36, 53.55(2C), 40.00, 28.83(2C). HRMS (ESI⁺) for $\text{C}_{27}\text{H}_{30}\text{FN}_7\text{O}_4$, $[\text{M}+\text{Na}]^+$ calcd: 558.2236, found: 558.2260.

4.2.1.7 *1-(2-((4-((4-((3-acrylamidophenyl)amino)-5-fluoropyrimidin-2-yl)amino)phenyl)amino)-2-oxoethyl)-N-hydroxypiperidine-4-carboxamide (10g)*

Yield 15.1%; off-white solid. ^1H NMR(400 MHz, DMSO- d_6): δ 10.42(s, 1H), 10.17(s, 1H), 9.46(s, 1H), 9.41(s, 1H), 9.12(s, 1H), 8.70(s, 1H), 8.10(d, $J=3.48$ Hz, 1H), 7.99(s, 1H), 7.61(d, $J=8.78$ Hz, 2H), 7.56(d, $J=8.49$ Hz, 1H), 7.45–7.42(m, 3H), 7.28(t, $J=8.05$ Hz, 1H), 6.49(dd, $J=16.84, 10.00$ Hz, 1H), 6.28(dd, $J=16.84, 1.21$ Hz, 1H), 5.77(dd, $J=10.00, 1.21$ Hz, 1H), 3.07(s, 2H), 2.91(d, $J=10.35$ Hz, 2H), 2.13(t, $J=10.61$ Hz, 2H), 2.02–1.96(m, 1H), 1.79–1.70(m, 2H), 1.62–1.59(m, 2H); ^{13}C NMR(100 MHz, DMSO- d_6): δ 171.96, 168.25, 163.61, 155.95(d, $J=1.80$ Hz), 150.20(d, $J=10.65$ Hz), 141.15(d, $J=19.79$ Hz), 140.96(d, $J=245.15$ Hz), 139.60(2C), 137.11, 132.48, 132.44, 129.03, 127.19, 120.38(2C), 119.21(2C), 117.73, 115.12, 113.61, 62.54(2C), 53.31, 40.91, 28.78(2C). HRMS (ESI⁺) for $\text{C}_{27}\text{H}_{29}\text{FN}_8\text{O}_4$, $[\text{M}+\text{Na}]^+$ calcd: 571.2188, found: 571.2191.

4.2.1.8 *1-(4-((4-((2-acrylamidophenyl)amino)-5-chloropyrimidin-2-yl)amino)phenyl)-N-hydroxypiperidine-4-carboxamide (10h)*

Yield 20.5%; off-white solid. ^1H NMR (400 MHz, DMSO- d_6): δ 10.46(s, 1H), 10.23(s, 1H),

9.05(s, 1H), 8.73(s, 1H), 8.45(s, 1H), 8.07(s, 1H), 7.78(d, $J=7.81$ Hz, 1H), 7.44(d, $J=7.80$ Hz, 1H), 7.38(d, $J=8.32$ Hz, 2H), 7.33(t, $J=7.69$ Hz, 1H), 7.26(t, $J=7.50$ Hz, 1H), 6.74(d, $J=8.35$ Hz, 2H), 6.52(dd, $J=17.01, 10.21$ Hz, 1H), 6.34(dd, $J=17.01$, 1H), 5.81(dd, $J=10.21$ Hz, 1H), 3.57(d, $J=11.91$ Hz, 2H), 2.54(td, $J=10.75, 3.84$ Hz, 1H), 2.13–2.09(m, 2H), 1.74–1.68(m, 4H); ^{13}C NMR(100 MHz, DMSO- d_6): δ 171.87, 164.74, 158.35, 156.41, 154.90, 146.88, 132.96, 132.27, 131.60, 131.44, 128.15, 127.63, 126.07, 125.77, 125.00, 120.66(2C), 116.78(2C), 103.80, 49.77(2C), 40.00, 28.60(2C). HRMS (ESI $^+$) for $\text{C}_{25}\text{H}_{26}\text{ClN}_7\text{O}_3$, $[\text{M}+\text{Na}]^+$ calcd: 530.1678, found: 530.1687.

4.2.1.9 *1-(4-((4-((2-acrylamidophenyl)amino)-5-chloropyrimidin-2-yl)amino)benzyl)-N-hydroxy piperidine-4-carboxamide (10i)*

Yield 11.0%; off-white solid. ^1H NMR(400 MHz, DMSO- d_6): δ 10.38(s, 1H), 10.20(s, 1H), 9.27(s, 1H), 8.68(s, 1H), 8.52(s, 1H), 8.12(s, 1H), 7.76(d, $J=7.60$ Hz, 1H), 7.48(d, $J=8.16$ Hz, 3H), 7.32(t, $J=7.20$ Hz, 1H), 7.28(t, $J=7.56$ Hz, 1H), 7.03(d, $J=8.28$ Hz, 2H), 6.52(dd, $J=16.92, 10.12$ Hz, 1H), 6.34(dd, $J=16.92, 1.36$ Hz, 1H), 5.82(dd, $J=10.12, 1.36$ Hz, 1H), 3.33(s, 2H), 2.80(d, $J=10.76$ Hz, 2H), 1.98–1.93(m, 1H), 1.86–1.82(m, 2H), 1.63–1.56(m, 4H); ^{13}C NMR(100 MHz, DMSO- d_6): δ 172.04, 164.74, 158.22, 156.58, 154.95, 139.61, 132.50, 131.95, 131.47, 131.37, 129.25(2C), 128.20, 127.96, 125.97(2C), 124.94, 119.14(2C), 104.45, 62.43, 52.97(2C), 40.00, 28.89(2C).

4.2.1.10 *1-(2-(4-((4-((2-acrylamidophenyl)amino)-5-chloropyrimidin-2-yl)amino)phenoxy)ethyl)-N-hydroxypiperidine-4-carboxamide (10j)*

Yield 13.3%; off-white solid. ^1H NMR(400 MHz, DMSO- d_6): δ 10.39(s, 1H), 10.22(s, 1H), 9.12(s, 1H), 8.70(s, 1H), 8.47(s, 1H), 8.08(s, 1H), 7.75(d, $J=7.76$ Hz, 1H), 7.46(d, $J=7.86$ Hz, 1H),

7.43(d, $J=8.04$ Hz, 2H), 7.34(t, $J=7.49$ Hz, 1H), 7.27(t, $J=7.56$ Hz, 1H), 6.72(d, $J=8.05$ Hz, 2H), 6.52(dd, $J=16.88, 10.00$ Hz, 1H), 6.34(d, $J=16.88$ Hz, 1H), 5.82(d, $J=10.00$ Hz, 1H), 3.98(t, $J=5.23$ Hz, 2H), 2.95(d, $J=10.71$ Hz, 2H), 2.63(t, $J=5.23$ Hz, 2H), 1.99–1.96(m, 3H), 1.63–1.58(m, 4H); ^{13}C NMR(100 MHz, DMSO- d_6): δ 171.99, 164.73, 158.30, 156.48, 153.67, 134.04, 132.17, 131.76, 131.44, 128.18, 127.79, 126.06, 125.89, 124.95, 120.93(2C), 114.62(2C), 103.97, 66.22, 57.42, 53.62(2C), 40.00, 28.93(2C). HRMS (ESI $^+$) for $\text{C}_{27}\text{H}_{30}\text{ClN}_7\text{O}_4$, $[\text{M}+\text{Na}]^+$ calcd: 574.1940, found: 574.1954.

4.2.1.11 *1-(2-(((4-(((2-acrylamidophenyl)amino)-5-chloropyrimidin-2-yl)amino)phenyl)amino)-2-oxoethyl)-N-hydroxypiperidine-4-carboxamide (10k)*

Yield 12.9%; off-white solid. ^1H NMR(400 MHz, DMSO- d_6): δ 10.42(s, 1H), 10.20(s, 1H), 9.52(s, 1H), 9.25(s, 1H), 8.71(s, 1H), 8.51(s, 1H), 8.11(s, 1H), 7.77(d, $J=7.43$ Hz, 1H), 7.48(d, $J=7.70$ Hz, 3H), 7.38(d, $J=8.59$ Hz, 2H), 7.30(t, $J=8.48$ Hz, 2H), 6.34(dd, $J=16.97, 10.24$ Hz, 1H), 6.53(dd, $J=16.97$ Hz, 1H), 5.81(d, $J=10.24$ Hz, 1H), 3.11(s, 2H), 2.93–2.90(d, $J=9.61$ Hz, 2H), 2.16(t, $J=11.53$ Hz, 2H), 2.01–1.98(m, 1H), 1.80–1.70(m, 2H), 1.63–1.60(m, 2H); ^{13}C NMR(100 MHz, DMSO- d_6): δ 171.92, 168.12, 164.74, 158.14, 156.56, 154.93, 136.63, 132.72, 132.13, 131.91, 131.45, 128.19, 127.88, 125.95(2C), 124.97, 120.24(2C), 119.38(2C), 104.31, 62.34, 53.25(2C), 39.21, 28.64(2C). HRMS (ESI $^+$) for $\text{C}_{27}\text{H}_{29}\text{ClN}_8\text{O}_4$, $[\text{M}+\text{Na}]^+$ calcd: 587.1893, found: 587.1908.

4.2.1.12 *1-(4-(((4-(((2-acrylamidophenyl)amino)-5-chloropyrimidin-2-yl)amino)benzyl)-N-hydroxypiperidine-4-carboxamide (10l)*

Yield 9.4%; off-white solid. ^1H NMR(400 MHz, DMSO- d_6): δ 10.38(s, 1H), 10.17(s, 1H),

9.27(s, 1H), 8.80(s, 1H), 8.70(s, 1H), 8.11(s, 1H), 7.68(d, $J=8.82$ Hz, 2H), 7.62(d, $J=8.22$ Hz, 2H), 7.55(d, $J=8.10$ Hz, 2H), 7.08(d, $J=8.16$ Hz, 2H), 6.47(dd, $J=16.92, 10.06$ Hz, 1H), 6.29(dd, $J=16.92, 1.74$ Hz, 1H), 5.77(dd, $J=10.06, 1.74$ Hz, 1H), 3.33(s, 2H), 2.79(d, $J=10.98$ Hz, 2H), 1.96–1.91(m, 1H), 1.84–1.81(m, 2H), 1.59–1.55(m, 4H); ^{13}C NMR(100 MHz, DMSO- d_6): δ 172.03, 163.46, 158.20, 156.42, 154.83, 139.67, 135.62, 134.66, 132.41, 131.43, 129.33(2C), 127.11, 124.20(2C), 119.84(2C), 119.28(2C), 104.23, 62.51, 52.96(2C), 40.00, 28.89(2C). HRMS (ESI⁺) for C₂₆H₂₈ClN₇O₃, [M+H]⁺ calcd: 522.2015, found: 522.2050.

4.2.1.13 *1-(2-(4-((4-((4-acrylamidophenyl)amino)-5-chloropyrimidin-2-yl)amino)phenoxy)ethyl)-N-hydroxypiperidine-4-carboxamide (10m)*

Yield 14.3%; off-white solid. ^1H NMR(400 MHz, DMSO- d_6): δ 10.39(s, 1H), 10.17(s, 1H), 9.12(s, 1H), 8.77(s, 1H), 8.69(s, 1H), 8.07(s, 1H), 7.66(d, $J=8.64$ Hz, 2H), 7.59(d, $J=7.15$ Hz, 2H), 7.47(d, $J=8.30$ Hz, 2H), 6.77(d, $J=8.58$ Hz, 2H), 6.45(dd, $J=16.94, 10.16$ Hz, 1H), 6.28(dd, $J=16.94, 1.14$ Hz, 1H), 5.77(dd, $J=10.16, 1.14$ Hz, 1H), 3.98(t, $J=5.70$ Hz, 2H), 2.94(d, $J=11.16$ Hz, 2H), 2.63(t, $J=5.70$ Hz, 2H), 1.98–1.93(m, 3H), 1.62–1.57(m, 4H); ^{13}C NMR(100 MHz, DMSO- d_6): δ 171.96, 163.43, 158.32, 156.42, 154.92, 153.78, 135.57, 134.70, 134.05, 132.39, 127.09, 124.29(2C), 121.26(2C), 119.84(2C), 114.60(2C), 103.61, 66.16, 57.48, 53.62(2C), 40.00, 28.93(2C). HRMS (ESI⁺) for C₂₇H₃₀ClN₇O₄, [M+H]⁺ calcd: 552.2121, found: 552.2138.

4.2.1.14 *1-(2-((4-((4-((4-acrylamidophenyl)amino)-5-chloropyrimidin-2-yl)amino)phenyl)amino)-2-oxoethyl)-N-hydroxypiperidine-4-carboxamide (10n)*

Yield 12.5%; off-white solid. ^1H NMR(400 MHz, DMSO- d_6): δ 10.43(s, 1H), 10.18(s, 1H),

9.52(s, 1H), 9.25(s, 1H), 8.72(s, 1H), 8.71(s, 1H), 8.12(s, 1H), 7.69–7.64(m, 4H), 7.55(d, $J=8.63$ Hz, 2H), 7.44(d, $J=8.60$ Hz, 2H), 6.47(dd, $J=16.90, 10.00$ Hz, 1H), 6.27(dd, $J=16.90, 2.10$ Hz, 1H), 5.76(dd, $J=10.00, 2.10$ Hz, 1H), 3.09(s, 2H), 2.90(d, $J=11.0$ Hz, 2H), 2.14(t, $J=11.4$ Hz, 2H), 2.02–1.94(m, 1H), 1.75(qd, $J=12.2$ Hz, 2H), 1.60(dd, $J=11.66$ Hz, 2H); ^{13}C NMR(100 MHz, DMSO- d_6): δ 171.96, 168.29, 163.45, 158.15, 156.29, 154.81, 136.73, 135.54, 134.70, 132.78, 132.42, 127.11, 123.89(2C), 120.43(2C), 119.84(2C), 119.59(2C), 104.17, 62.46, 53.30(2C), 39.28, 28.72(2C). HRMS (ESI $^+$) for $\text{C}_{27}\text{H}_{29}\text{ClN}_8\text{O}_4$, $[\text{M}+\text{Na}]^+$ calcd: 587.1893, found: 587.1940.

4.2.2 General procedure for the synthesis of **10o~q**

A mixture of **15a~d** (3.0 mmol), **18a~d** (1.5 mmol), and *p*-TsOH (4.5 mmol) in ethyl alcohol was gradually heated to 70 °C and stirred for 3 h. After reaction, the solvent was vacuum distilled and the residuum was dispersed with saturated sodium bicarbonate/ethyl acetate. The crude product was purified using flash chromatography with dichloromethane/methanol as eluents.

4.2.1.15 ethyl 1-(4-((4-((2-acrylamidophenyl)amino)-5-chloropyrimidin-2-yl)amino)phenyl) piperidine-4-carboxylate (**10o**)

Yield 60.2%; off-white solid. ^1H NMR(400 MHz, DMSO- d_6): δ 10.23(s, 1H), 9.07(s, 1H), 7.46(s, 1H), 8.07(s, 1H), 7.78(d, $J=7.92$ Hz, 1H), 7.44(d, $J=7.56$ Hz, 1H), 7.38(d, $J=8.40$ Hz, 2H), 7.34(td, $J=7.86, 1.20$ Hz, 1H), 7.27(td, $J=7.98, 1.08$ Hz, 1H), 6.73(d, $J=8.76$ Hz, 2H), 6.52(dd, $J=16.98, 10.20$ Hz, 1H), 6.33(dd, $J=16.98, 1.62$ Hz, 1H), 5.81 (dd, $J=10.20, 1.62$ Hz, 1H), 4.08(q, $J=7.14$ Hz, 2H), 3.47(dt, $J=12.42, 3.17$ Hz, 2H), 2.64(td, $J=12.06, 2.28$ Hz, 2H), 2.43(tt, $J=11.22, 3.84$ Hz, 1H), 1.89(dd, $J=13.20, 2.94$ Hz, 2H), 1.66(qd, $J=11.64, 3.84$ Hz, 2H), 1.19(t, $J=7.14$ Hz,

3H); ^{13}C NMR(100 MHz, $\text{DMSO}-d_6$): δ 174.76, 164.72, 158.34, 156.40, 154.89, 146.60, 133.06, 132.25, 131.61, 131.44, 128.16, 127.65, 126.05, 125.76, 124.98, 120.61, 116.85, 103.82, 60.32, 49.45, 40.56, 28.17, 14.57. HRMS (ESI⁺) for $\text{C}_{27}\text{H}_{29}\text{ClN}_6\text{O}_3$, $[\text{M}+\text{Na}]^+$ calcd: 543.1882, found: 543.1881.

4.2.1.16 ethyl 1-(4-((4-((2-acrylamidophenyl)amino)-5-chloropyrimidin-2-yl)amino)benzyl) piperidine-4-carboxylate (10p)

Yield 56.3%; off-white solid. ^1H NMR(400 MHz, $\text{DMSO}-d_6$): δ 10.21(s, 1H), 9.28(s, 1H), 8.52(s, 1H), 8.12(s, 1H), 7.74(dd, $J=7.98$, 1.21 Hz, 1H), 7.47(dd, $J=7.98$, 1.21 Hz, 1H), 7.46(d, $J=8.42$ Hz, 2H), 7.32(td, $J=7.51$, 1.40 Hz, 1H), 7.27(td, $J=7.51$, 1.40 Hz, 1H), 7.00(d, $J=8.42$ Hz, 2H), 6.51(dd, $J=17.02$, 10.21 Hz, 1H), 6.32(dd, $J=17.02$, 1.74 Hz, 1H), 5.80(dd, $J=10.21$, 1.74 Hz, 1H), 4.05(q, $J=7.08$ Hz, 2H), 3.31(s, 2H), 2.70(d, $J=10.74$ Hz, 2H), 2.26(tt, $J=11.06$, 3.84 Hz, 1H), 1.92(t, $J=10.80$ Hz, 2H), 1.77(d, $J=12.96$ Hz, 2H), 1.53(qd, $J=11.22$, 3.42 Hz, 2H), 1.19(t, $J=7.08$ Hz, 3H); ^{13}C NMR(100 MHz, $\text{DMSO}-d_6$): δ 174.90, 164.70, 158.19, 156.56, 154.95, 132.03, 131.95, 131.45, 129.23(2C), 128.21, 127.98, 125.96(2C), 124.89, 119.08(2C), 104.41, 62.38, 60.24, 52.55(2C), 40.81, 28.46(2C), 14.57. HRMS (ESI⁺) for $\text{C}_{28}\text{H}_{31}\text{ClN}_6\text{O}_3$, $[\text{M}+\text{H}]^+$ calcd: 535.2219, found: 535.2220.

4.2.1.17 ethyl 1-(4-((4-((3-acrylamidophenyl)amino)-5-chloropyrimidin-2-yl)amino)benzyl) piperidine-4-carboxylate (10q)

Yield 61.4%; off-white solid. ^1H NMR(400 MHz, $\text{DMSO}-d_6$): δ 10.18(s, 1H), 9.30(s, 1H), 8.94(s, 1H), 8.13(s, 1H), 7.89(s, 1H), 7.55–7.52(m, 3H), 7.33–7.30(m, 2H), 7.00 (d, $J=8.28$ Hz, 2H), 6.45(dd, $J=16.95$, 10.14 Hz, 1H), 6.26(dd, $J=16.95$, 1.80 Hz, 1H), 5.74(dd, $J=10.14$, 1.80 Hz, 1H), 4.04(q, $J=7.08$ Hz, 2H), 3.28(s, 2H), 2.69(d, $J=10.86$ Hz, 2H), 2.24(tt, $J=11.22$, 3.84 Hz, 1H), 1.89(t,

$J=10.98$ Hz, 2H), 1.75(dd, $J=12.84$, 3.00 Hz, 2H), 1.52(qd, $J=11.14$, 3.42 Hz, 2H), 1.16(t, $J=7.08$ Hz, 3H); ^{13}C NMR(100 MHz, $\text{DMSO}-d_6$): δ 174.87, 163.57, 158.15, 156.63, 155.22, 139.59, 139.56, 139.28, 132.39, 131.31, 129.28(2C), 128.99, 127.23, 119.68, 119.07(2C), 115.91, 115.71, 104.13, 62.44, 60.20, 52.57(2C), 40.84, 28.45(2C), 14.55. HRMS (ESI⁺) for $\text{C}_{28}\text{H}_{31}\text{ClN}_6\text{O}_3$, $[\text{M}+\text{H}]^+$ calcd: 535.2219, found: 535.2241.

4.2.3 General procedure for the synthesis of **10r~t**

Applying with the general procedure 4.4 to synthesize the ester-intermediates, ester-intermediates (0.5 mmol) and 10% aq. sodium hydroxide in 1,4-dioxane/water, the mixture was stirred at room temperature for 5 h. After reaction, adjusted pH to 6 with dilute hydrochloric acid and distilled out 1,4-dioxane. Then, the precipitate was filtrated and washed with water to obtain **10r~t** which could directly be used without further purification.

4.2.1.18 1-(4-((4-((2-acrylamidophenyl)amino)-5-chloropyrimidin-2-yl)amino)phenyl)piperidine-4-carboxylic acid (**10r**)

Yield 62.1%; off-white solid. ^1H NMR(400 MHz, $\text{DMSO}-d_6$): δ 12.21(s, 1H), 10.21(s, 1H), 9.05(s, 1H), 8.45(s, 1H), 8.07(s, 1H), 7.77(d, $J=7.86$ Hz, 1H), 7.44(d, $J=7.80$ Hz, 1H), 7.37(d, $J=8.47$ Hz, 2H), 7.34(t, $J=7.50$ Hz, 1H), 7.27(t, $J=7.32$ Hz, 1H), 6.73(d, $J=8.56$ Hz, 2H), 6.51(dd, $J=16.99$, 10.22 Hz, 1H), 6.32(dd, $J=16.99$, 1.08 Hz, 1H), 5.80(dd, $J=10.22$, 1.08 Hz, 1H), 3.47(dt, $J=12.21$, 3.53 Hz, 2H), 2.63(td, $J=11.41$, 2.05 Hz, 2H), 2.34(tt, $J=11.16$, 3.66 Hz, 1H), 1.89(dd, $J=12.94$, 2.36 Hz, 2H), 1.64(qd, $J=11.20$, 3.54 Hz, 2H); ^{13}C NMR(100 MHz, $\text{DMSO}-d_6$): δ 176.48, 164.72, 158.34, 156.41, 154.90, 146.69, 133.01, 132.25, 131.61, 131.44, 128.17, 127.66, 126.07, 125.78, 124.98,

120.60(2C), 116.83(2C), 103.78, 49.57(2C), 40.56, 28.25(2C). HRMS (ESI⁺) for C₂₅H₂₅ClN₆O₃, [M+H]⁺ calcd: 493.1749, found: 193.1748.

4.2.1.19 *1-(4-((4-((2-acrylamidophenyl)amino)-5-chloropyrimidin-2-yl)amino)benzyl)piperidine-4-carboxylic acid (10s)*

Yield 45.3%; off-white solid. ¹H NMR(400 MHz, DMSO-*d*₆): δ 10.21(s, 1H), 9.27(s, 1H), 8.52(s, 1H), 8.11(s, 1H), 7.74(d, *J*=7.60 Hz, 1H), 7.47(d, *J*=7.60 Hz, 1H), 7.46(d, *J*=8.22 Hz, 2H), 7.32(td, *J*=7.44, 1.38 Hz, 1H), 7.27(td, *J*=7.56, 1.26 Hz, 1H), 7.01(d, *J*=8.35 Hz, 2H), 6.51(dd, *J*=16.98, 10.19 Hz, 1H), 6.32(dd, *J*=16.98, 1.68 Hz, 1H), 5.80(dd, *J*=10.19, 1.68 Hz, 1H), 3.33(s, 2H), 2.71(d, *J*=10.68 Hz, 2H), 2.16(tt, *J*=11.10, 3.66 Hz, 1H), 1.92(t, *J*=10.56 Hz, 2H), 1.76(d, *J*=12.01 Hz, 2H), 1.52(qd, *J*=11.12, 3.42 Hz, 2H); ¹³C NMR(100 MHz, DMSO-*d*₆): δ 176.62, 164.71, 158.20, 156.56, 154.94, 139.61, 132.06, 131.93, 131.45, 131.24, 129.28(2C), 128.18, 127.95, 125.96(2C), 124.90, 119.10(2C), 104.42, 62.37, 52.69(2C), 40.82, 28.48(2C). HRMS (ESI⁺) for C₂₆H₂₇ClN₆O₃, [M+Na]⁺ calcd: 529.1725, found: 529.1747.

4.2.1.20 *1-(4-((4-((3-acrylamidophenyl)amino)-5-chloropyrimidin-2-yl)amino)phenyl)piperidine-4-carboxylic acid (10t)*

Yield 51.4%; off-white solid. ¹H NMR(400 MHz, DMSO-*d*₆): δ 12.29(s, 1H), 10.30(s, 1H), 9.22(s, 1H), 8.89(s, 1H), 8.10(s, 1H), 7.93(s, 1H), 7.57(d, *J*=7.40 Hz, 1H), 7.48(d, *J*=8.20 Hz, 2H), 7.30(t, *J*=7.50 Hz, 1H), 7.27(d, *J*=7.45 Hz, 1H), 6.81(d, *J*=8.20 Hz, 2H), 6.50(dd, *J*=16.92, 10.20 Hz, 1H), 6.26(dd, *J*=16.92, 1.68 Hz, 1H), 5.76(dd, *J*=10.20, 1.68 Hz, 1H), 3.44(d, *J*=11.82 Hz, 2H), 2.79–2.66(m, 2H), 2.41–2.35(m, 1H), 1.91(t, *J*=11.10 Hz, 2H), 1.73–1.66(m, 2H); ¹³C NMR(100

MHz, DMSO- d_6): δ 176.33, 163.58, 158.08, 156.54, 155.03, 145.83, 139.58, 139.35, 132.47, 129.08, 127.34, 120.51(2C), 119.43, 117.43(2C), 115.90, 115.65, 103.72, 50.20(2C), 40.53, 28.03(2C).

HRMS (ESI⁺) for C₂₅H₂₆ClN₆O₃, [M+Na]⁺ calcd: 515.1569, found: 515.1532.

4.2.4 Synthetic method of **10u**

A mixture of **10o** (0.5 mmol) and 10% aq. sodium hydroxide in 1,4-dioxane/water was heated to 50 °C and stirred for 5 hours. After reaction, adjusted pH to 6 with dilute hydrochloric acid and distilled out 1,4-dioxane. Then, the precipitate was filtrated and washed with water to give **10u** which could directly be used without further purification.

4.2.1.21 1-(4-((5-chloro-4-((2-(3-methoxypropanamido)phenyl)amino)pyrimidin-2-yl)amino)phenyl)piperidine-4-carboxylic acid (**10u**)

Yield 82.1%; off-white solid. ¹H NMR(400 MHz, DMSO- d_6): δ 12.22(s, 1H), 9.99(s, 1H), 9.05(s, 1H), 8.39(s, 1H), 8.07(s, 1H), 7.73(d, J =7.80 Hz, 1H), 7.39(d, J =7.86 Hz, 1H), 7.36(d, J =7.98 Hz, 2H), 7.30(t, J =7.44 Hz, 1H), 7.24(t, J =7.14 Hz, 1H), 6.72(d, J =8.22 Hz, 2H), 3.60(t, J =6.00 Hz, 2H), 3.46(d, J =12.12 Hz, 2H), 3.20(s, 3H), 2.63(t, J =11.10 Hz, 2H), 2.59(t, J =6.00 Hz, 2H), 2.34(tt, J =11.10, 3.84 Hz, 1H), 1.89(d, J =12.88 Hz, 2H), 1.64(qd, J =11.24, 3.36 Hz, 2H); ¹³C NMR(100 MHz, DMSO- d_6): δ 176.49, 170.93, 158.33, 156.42, 154.83, 146.66, 133.04, 132.01, 131.93, 127.53, 125.76(2C), 124.79, 120.55(2C), 116.83(2C), 103.78, 68.65, 58.37, 49.58(2C), 40.00, 36.93, 28.26(2C). HRMS (ESI⁺) for C₂₆H₂₉ClN₆O₄, [M+H]⁺ calcd: 525.2012, found: 525.2002.

4.3 Kinase enzymatic assays

The ADP-Glo™ system (EGFR^{WT}, Catalog. V9261; EGFR^{T790M/L858R}, Catalog. V5325) were purchased from Promega Corporation (USA) and were used to perform the enzymatic assays. The experiments were performed according to the instructions of the manufacturer. The more detailed and complete protocols, and the active kinase data were available at: <https://www.promega.com.cn/resources/protocols/product-information-sheets/n/EGFR-kinase-enzyme-system-protocol/>. For all of the tested targets, concentrations consisting of suitable levels from 0.1 to 1000 nM were used. The test was performed in a 384-well plate, and includes the major steps below: (1) perform 5 µL kinase reaction using 1 × kinase buffer (e.g., 1 × reaction buffer A), (2) incubate at room temperature for 60 min, (3) add 5 µL of ADP-Glo™ reagent to stop the kinase reaction and deplete the unconsumed ATP leaving only ADP and a very low background of ATP, (4) incubate at room temperature for 40 min, (5) add 10 µL of kinase detection, (6) reagent to convert ADP to ATP and introduce luciferase and luciferin to detect ATP, (7) incubate at room temperature for 30 min, (8) plate was measured on TriStar® LB942 Multimode Microplate Reader (BERTHOLD) to detect the luminescence (Integration time 0.5–1 s). Curve fitting and data presentations were performed using GraphPad Prism version 5.0.

4.4 Cell activity assay

A 431, A 549, Aspc-1, and H 23 cells were obtained from the American Type Culture Collection. H 1975, HBE and L-02 cells were purchased from Fuheng Biology Company (Shanghai, China). H 1975, Aspc-1, H 23, and A 549 cells were grown in RPMI-1640 (Gibco®, USA) supplemented with 10 % FBS (Gibco®, USA), 1 % penicillin-streptomycin (Beyotime Company, China). A 431, HBE

and L-02 cells were grown in DMEM (Gibco®, USA) supplemented with 10 % FBS (Gibco®, USA), 1 % penicillin-streptomycin (Beyotime Company, China). All cells were maintained and propagated as monolayer cultures at 37 °C in humidified 5 % CO₂ incubator. The Cell Counting Kit-8 (CCK-8) reagent was purchased from Biotool Company (Switzerland). Cell viability was assessed by the CCK-8 assay based on the reduction of CCK-8 by succinate dehydrogenases of viable cells to a yellow formazan product. Cells were grown in 96-well culture plates (3000–4000/well) for 12 h before compounds of various concentrations (1.25 to 40 µM) were added. Cell proliferation was determined after treatment with compounds for 72 h. Subsequently, 10 µL of CCK-8 reagent (Biotool Company, Switzerland, 5.0 mg/mL) dissolved in the medium was added and the cells were incubated for another 1–2 h at 37 °C. The absorbance was measured at 450 nm with a microplate reader (Thermo Fisher, USA). All doses were tested in triplicates and the experiment was repeated at least three times. IC₅₀ values were calculated using GraphPad Prism version 5.0.

4.5 Wound-Healing Assay

The cancer cells were cultured in 6-well plates for 48 h at 37 °C. The injury lines were created in the cell monolayer and washed with PBS to remove cell debris, then the cells were treated with **10j** (1 and 4 µM) for 0, 24, and 48 h. After that, the dead cells were washed away with PBS, and the images were photographed by the fluorescence microscope (OLYMPUS, Tokyo, Japan).

4.6 DAPI staining Assays

Approximately 2×10^5 cells/well of H1975 cells in 6-well plates were incubated in an incubator for 12 h, then treated with different concentrations of inhibitors (0.25, 1, and 4 µM) for 72 h. After

incubation, the cells were washed with PBS twice. DAPI staining was performed after being treated as mentioned above. The cells plated in 6-well plates were washed twice with PBS and fixed with 10 % formaldehyde for 10 min, then washed with PBS three times. Cells were subsequently incubated in DAPI (1.0 $\mu\text{g}/\text{mL}$) solution at room temperature for 10 min, washed with PBS and examined under a fluorescence microscope (OLYMPUS, Tokyo, Japan).

4.7 Flow cytometry assay

The Annexin V-FITC Apoptosis Detection Kit and Cell Cycle Assay were all purchased from Beyotime Company (Shanghai, China). Compounds-induced apoptotic cell death was further quantitated by Annexin V-propidium iodide assay. Briefly, after treatment with different concentrations of compounds for 48 h, the cells were collected and washed twice with ice-cold PBS, cells then resuspended in binding buffer with Annexin-V and PI and incubated at room temperature for 15 min in the dark. The stained cells were analyzed using flow cytometry (Beckman, USA). The H1975 (1×10^6 cells/well) incubated in 6-well plates were treated with solvent control (DMSO), **10j** in medium containing 5% FBS for 72 h. Then, collected and fixed with 70% ethanol at 4 °C overnight. After being fixed with 70% ethanol at 4 °C, the cells were stained with Annexin V-FITC (5 μL)/propidium iodide (5 μL), and analyzed by flow cytometry assay (Becton-Dickinson, USA).

Cell cycle distribution was evaluated by flow cytometry. The cells at a density of approximately 2×10^5 cells/well were incubated in 6-well plates, treated with different concentrations of **10j** for 48 h, collected and fixed with 70% ice-cold ethanol at 4 °C overnight. Following this, cells were stained with 500 μL PBS containing 50 mg/mL propidium iodide and 0.5 mg/mL RNase for 30 min at 37 °C.

The DNA content was analyzed on a flow cytometer (Beckman, USA).

4.8 Mouse tumor xenograft efficacy study

The STOCK-Foxn1^{nu/Nju} nude mice weighing 25~30 g in ~6 weeks old. All animals were housed in a controlled environment at 23 ± 2 °C under a 12 h dark/light cycle with free access to food and water. The animal maintenance and experiments were performed in accordance with the guidelines of the Animal Care and Use Committee. H1975 cells (3×10^6) were suspended in 0.1 mL of PBS and injected subcutaneously into the right oter region of the mice. Three days after implantation, the mice were randomly divided into seven groups in which the mice in control group were received by oral 25% PEG-400, and the mice in other six groups were oral administrated with **10j** at the doses of 50 mg/kg for 14 days. At the end of the test, the animals were sacrificed and the tumors were obtained, photographed and weighted.

4.9 Molecular docking study

AutoDock 4.2.6 software was used to carry out the docking studies. Generally, the crystal structure (PDB: 3IKA) of the kinase domain of EGFR^{T790M/L858R} bound to WZ4002 was used in the docking studies. The enzyme preparation and the hydrogen atoms adding was performed in the prepared process. The whole EGFR enzyme was defined as a receptor and the site sphere was selected on the basis of the binding location of WZ4002. By moving WZ4002 and the irrelevant water, molecule **10j** was introduced. The binding interaction energy was calculated to include Van der Waals, electrostatic, and torsional energy terms defined in the tripos force field. The structure optimization was performed using a genetic algorithm, and only the best-scoring ligand protein complex was kept

for analyses and presented by PyMOL software.

Acknowledgements

This work was supported by the "innovative research team in SYPHU by the supporting fund for universities from the Chinese Central Government (51150039)", Research Fund of Higher Education of Liaoning Province (LQ2019004), Science and Technology Innovation Fund of Dalian, Liaoning province, China (2020JJ27SN072), "Xing Liao" Talents Project of Liaoning Province, China (XLYC1807011), Liaoning Province Ph.D. Research Start-up Fund (2020-BS-199), and Scientific Research Fund of Liaoning Province Education Administration (LZ2020041).

References

- [1] J.J. Lin and A.T. Shaw, Resisting Resistance: Targeted Therapies in Lung Cancer, *Trends Cancer* 2 (2016) 350–364.
- [2] B.P. Ceresa, J.L. Peterson, *Cell and Molecular Biology of Epidermal Growth Factor Receptor*, *Int. Rev. Cel. Mol. Bio*, 313 (2014) 145–178.
- [3] Y. Yarden, G. Pines, The ERBB network: at last, cancer therapy meets systems biology, *Nat. Rev. Cancer* 12 (2012) 553–563.
- [4] Z. Yang, N. Yang, Q. Ou, Y. Xiang, T. Jiang, X. Wu, H. Bao, X. Tong, X. Wang, Y.W. Shao, Investigating novel resistance mechanisms to third-generation EGFR tyrosine kinase inhibitor osimertinib in non-small cell lung cancer patients, *Clin. Cancer Res.* 24 (2018) 3097–3107.
- [5] B. Han, S. Tjulandin, K. Hagiwara, N. Normanno, L. Wulandari, K. Laktionov, A. Hudoyo, Y. He, Y.P. Zhang, M.Z. Wang, EGFR mutation prevalence in Asia-Pacific and Russian patients with

advanced NSCLC of adenocarcinoma and nonadenocarcinoma histology: the IGNITE study, *Lung Cancer* 113 (2017) 37–44.

[6] C.H. Yun, T.J. Boggon, Y.q. Li, M.S. Woo, H. Greulich, M. Meyerson, M.J. Eck, Structures of lung cancer-derived EGFR mutants and inhibitor complexes: Mechanism of activation and insights into differential inhibitor sensitivity, *Cancer Cell* 11 (2007) 217–227.

[7] X. Zhang, J. Gureasko, K. Shen, P.A. Cole, J. Kuriyan, An allosteric mechanism for activation of the kinase domain of epidermal growth factor receptor, *Cell* 125 (2006) 1137–1149.

[8] S.K. Chan, W.J. Gullick, M.E. Hill, Mutations of the epidermal growth factor receptor in non-small cell lung cancer—Search and destroy, *Eur. J. Cancer* 42 (2006) 17–23.

[9] H. Shigematsu, A.F. Gazdar, Somatic mutations of epidermal growth factor receptor signaling pathway in lung cancers, *Int. J. Cancer* 118 (2006) 257–262.

[10] T.J. Lynch, D.W. Bell, R. Sordella, S. Gurubhagavatula, R.A. Okimoto, B.W. Brannigan, P.L. Harris, S.M. Haserlat, J.G. Supko, F.G. Haluska, D.N. Louis, D.C. Christiani, J. Settleman, D.A. Haber, Activating mutations in the epidermal growth factor receptor underlying responsiveness of non-small-cell lung cancer to gefitinib, *New. Engl. J. Med.* 350 (2004) 2129–2139.

[11] P. Bonomi, Erlotinib: a new therapeutic approach for non-small cell lung cancer, *Expert Opin. Investig. Drugs* 12 (2003) 1395–1401.

[12] Z.W. Yu, T.J. Boggon, S. Kobayashi, C. Jin, P.C. Ma, A. Dowlati, J.A. Kern, D.G. Tenen, B. Halmos, Resistance to an irreversible epidermal growth factor receptor (EGFR) inhibitor in EGFR-mutant lung cancer reveals novel treatment strategies, *Cancer Res.* 67 (2007) 10417–10427.

- [13] H.A. Yu, M.E. Arcila, N. Rekhtman, C.S. Sima, M.F. Zakowski, W. Pao, M.G. Kris, V.A. Miller, M. Ladanyi, G.J. Riely, Analysis of tumour specimens at the time of acquired resistance to EGFR-TKI therapy in 155 patients with EGFR-mutant lung cancers. *Clin. Cancer Res.* 19 (2013) 2240–2247.
- [14] C.H. Yun, K.E. Mengwasser, A.V. Toms, M.S. Woo, H. Greulich, K.K. Wong, M. Meyerson, M.J. Eck, The T790M mutation in EGFR kinase causes drug resistance by increasing the affinity for ATP, *P. Natl. Acad. Sci. USA* 105 (2008) 2070–2075.
- [15] D.N. Li, T. Shimamura, H.B. Ji, L. Chen, H.J. Haringsma, K. McNamara, M.C. Liang, S.A. Perera, S. Zaghlul, C.L. Borgman, S. Kubo, M. Takahashi, Y.P. Sun, L.R. Chirieac, R.F. Padera, N.I. Lindeman, P.A. Jänne, R.K. Thomas, M.L. Meyerson, M.J. Eck, J.A. Engelman, G.I. Shapiro, K.K. Wong, Bronchial and peripheral murine lung carcinomas induced by T790M-L858R mutant EGFR respond to HKI-272 and rapamycin combination therapy, *Cancer Cell* 12 (2007) 81–93.
- [16] D. Li, L. Ambrogio, T. Shimamura, S. Kubo, M. Takahashi, L.R. Chirieac, R.F. Padera, G.I. Shapiro, A. Baum, F. Himmelsbach, W.J. Rettig, M. Meyerson, F. Solca, H. Greulich, K.K. Wong, BIBW2992, an irreversible EGFR/HER2 inhibitor highly effective in preclinical lung cancer models. *Oncogene* 27 (2008) 4702–4711.
- [17] K.K. Wong, HKI-272 in non small cell lung cancer. *Clin. Cancer Res.* 13 (2007) s4593–s4596.
- [18] M.L. Sos, H.B. Rode, S. Heynck, M. Peifer, F. Fischer, S. Klüter, V.G. Pawar, C. Reuter, J.M. Heuckmann, J. Weiss, L. Ruddigkeit, M. Rabiller, M. Koker, J.R. Simard, M. Getlik, Y. Yuza, T.H. Chen, H. Greulich, R.K. Thomas, D Rauh, Chemogenomic Profiling Provides Insights into the

Limited Activity of Irreversible EGFR Inhibitors in Tumor Cells Expressing the T790M EGFR Resistance Mutation, *Cancer Res.* 70 (2010) 868–874.

[19] W. Zhou, D. Ercan, L. Chen, C.H. Yun, D. Li, M. Capelletti, A.B. Cortot, L. Chirieac, R.E. Iacob, R. Padera, J.R. Engen, K.K. Wong, M.J. Eck, N.S. Gray, P.A. Janne, Novel mutant-selective EGFR kinase inhibitors against EGFR T790M, *Nature* 462 (2009) 1070–1074.

[20] M.R. Finlay, M. Anderton, S. Ashton, P. Ballard, P.A. Bethel, M.R. Box, R.H. Bradbury, S.J. Brown, S. Butterworth, A. Campbell, C. Chorley, N. Colclough, D.A. Cross, G.S. Currie, M. Grist, L. Hassall, G.B. Hill, D. James, M. James, P. Kemmitt, T.K. linowska, G. Lamont, S.G. Lamont, N. Martin, H.L. McFarland, M.J. Mellor, J.P. Orme, D. Perkins, P. Perkins, G. Richmond, P. Smith, R.A. Ward, M.J. Waring, D. Whittaker, S. Wells, G.L. Wrigley, Discovery of a potent and selective EGFR inhibitor (AZD9291) of both sensitizing and T790M resistance mutations that spares the wild type form of the receptor, *J. Med. Chem.* 57 (2014) 8249–8267.

[21] J.C.H. Yang, D.R. Camidge, C.T. Yang, J.Y. Zhou, R.H. Guo, C.H. Chiu, G.C. Chang, H.S. Shiah, Y. Chen, C.C. Wang, D. Berz, W.C. Su, N. Yang, Z.P. Wang, J. Fang, J.H. Chen, P. Nikolinakos, Y. Lu, H.M. Pan, A. Maniam, L. Bazhenova, K. Shirai, M. Jahanzeb, M. Willis, N. Masood, N. Chowhan, T.C. Hsia, H. Jian, S. Lu, J. Thorac. *Oncol.* 15 (2020) 1907–1918.

[22] L.X. Chen, F.Y. Chi, T. Wang, N. Wang, W. Li, K.X. Liu, X.H. Shu, X.D. Ma, Y.J. Xu, The synthesis of 4-arylamido-2-arylamino-primidines as potent EGFR T790M/L858R inhibitors for NSCLC, *Bioorg. Med. Chem.* 26 (2018) 6087–6095.

[23] Z. Song, S. Huang, H. Yu, Y. Jiang, C. Wang, Q. Meng, X. Shu, H. Sun, K. Liu, Y. Li, X.D. Ma,

Synthesis and biological evaluation of morpholine-substituted diphenylpyrimidine derivatives (Mor-DPPYs) as potent EGFR T790M inhibitors with improved activity toward the gefitinib-resistant non-small cell lung cancers (NSCLC), *Eur. J. Med. Chem.* 133 (2017) 329–339.

[24] A.R. Song, J.B. Zhang, Y. Ge, C.Y. Wang, Q. Meng, Z.Y. Tang, J.Y. Peng, K.X. Liu, Y.X. Li, X.D. Ma, C-2 (E)-4-(Styryl)aniline substituted diphenylpyrimidine derivatives (Sty-DPPYs) as specific kinase inhibitors targeting clinical resistance related EGFR T790M mutant, *Eur. J. Med. Chem.* 25 (2017) 2724–2729.

[25] M. Ai, C.Y. Wang, Z.Y. Tang, K.X. Liu, X.L. Sun, T.Y. Ma, Y.X. Li, X.D. Ma, L. Li, L.X. Chen Design and synthesis of diphenylpyrimidine derivatives (DPPYs) as potential dual EGFR T790M and FAK inhibitors against a diverse range of cancer cell lines, *Bioorg. Chem.* 94 (2020) 103408.

[26] Y.M. Zhu, X. Zheng, C.Y. Wang, X.L. Sun, H.J. Sun, T.Y. Ma, Y.X. Li, K.X. Liu, L.X. Chen, X.D. Ma, Synthesis and Biological Activity of Thieno[3,2-d]pyrimidines as Potent JAK3 Inhibitors for the Treatment of Idiopathic Pulmonary Fibrosis, *Bioorg. Med. Chem.* 28 (2020) 115254.

[27] F.Y. Chi, L.X. Chen, C.Y. Wang, L. Li, X.L. Sun, Y.J. Xu, T.Y. Ma, K.X. Liu, X.D. Ma, X.H. Shu, JAK3 inhibitors based on thieno[3,2-d]pyrimidine scaffold: design, synthesis and bioactivity evaluation for the treatment of B-cell lymphoma. *Bioorg. Chem.* 95 (2020) 103542.

[28] S. Li, B. Wu, C.Y. Wang, J.Y. Zhao, H.J. Sun, X.L. Sun, K.X. Liu, H. Yuan, L.X. Chen, X.D. Ma, Synthesis and biological activity of imidazole group-substituted arylaminopyrimidines (IAAPs) as potent BTK inhibitors against B-cell lymphoma and AML, *Bioorg. Chem.* 106 (2021) 104385.

